Chinese Chemical Letters 35 (2024) 109807

Contents lists available at ScienceDirect

Chinese Chemical Letters

journal homepage: www.elsevier.com/locate/cclet

On-surface photo-induced dechlorination

Yu He, Hao Jiang, Shaoxuan Yuan, Jiayi Lu, Qiang Sun*

Materials Genome Institute, Shanghai University, Shanghai 200444, China

ARTICLE INFO

Article history:
Received 18 January 2024
Revised 14 March 2024
Accepted 20 March 2024
Available online 22 March 2024

Keywords:
On-surface synthesis
Scanning probe microscopy
On-surface photochemistry
Dechlorination reaction

ABSTRACT

On-surface Ullmann-type reaction, or the dehalogenated coupling, is arguably the most pivotal reaction in on-surface synthesis for the fabrications of carbon nanostructures. Hitherto, the vast majority of works rely on activating the C-Br bond of aryl bromide which has a moderate bond dissociation energy. The C-Cl bond of aryl chloride has a higher dissociation energy and requires much higher thermal energy to break the bond. In this study, we have explored the on-surface photo-induced dechlorination and achieved the activation of three distinct aryl chlorines on the Au(111) surface with mild temperatures. This work enriches our understanding of on-surface photo-induced reactions and highlights the potential of photochemistry in realizing unconventional reactions.

On-surface synthesis has proven to be versatile in fabricating covalently bonded nanoarchitectures with atomic precisions [1–4]. Among various reactions explored on surfaces, the Ullmann-type coupling, which traditionally refers to the coupling reaction between aryl halides catalyzed by transitional metals like copper, is arguably the most successfully and widely employed reaction in on-surface synthesis [4,5]. By harnessing the chemical catalysis of the metal surfaces [6–8], it facilitates the dissociation of C-X (X represents halogen atoms such as Cl, Br, I) bonds of molecular precursors and the following formation of C-C bonds [9–12]. The positions of the halogen atoms in the precursor determine where new covalent bonds will be formed, thereby inherently deciding the final structure [11,13,14]. Thanks to the on-surface Ullmann-type coupling, various carbon nanostructures with atomic precisions have been realized, including graphene nanoribbons of different topological structures [15–24], cycloparaphenylene and polyphenylene [25,26], coronoid [27,28], carbon-based organometallic hybrids [29,30] and nonbenzenoid carbon allotropes [31].

The advantages of the Ullmann-type reaction lie in its accuracy in constructing target carbon nanostructures, and different activations can be employed to trigger the reaction. Heat is so far the most commonly employed excitation for activating chemical reactions. However, thermal annealing sometimes faces challenges in achieving high chemical selectivity and leads to occurrence of defects [32], especially for those that require high temperatures. For instance, on-surface dechlorination requires a much higher activation temperature than the debrominations [33,34]. The high temperatures activate cyclodehydrogenation before dehalogenation and polymerization, leading to unexpected diverse products [35].

While heat remains the preferred stimulus, there are alternative activations available, such as scanning tunnelling microscope (STM) tip manipulation [36–39], electron beam [40], or light [41]. Among these alternative activations, light offers several advantages over the others. The adjustable parameters of wavelength, light flux and polarization enable possibilities to control reactions. Moreover, photocatalysis facilitates the activation of reactions at milder conditions than conventional thermal methods, utilizing sustainable and environmentally friendly energy source. It is noteworthy that photochemistry can give rise to the formation of species at excited state, subsequently introducing new reaction pathways. Thus, an increasing number of works are embracing light as an alternative tool to heat for triggering on-surface reactions [41–46]. On-surface photochemical reactions predominantly proceed *via* three underlying mechanisms: direct excitation, indirect excitation and charge transfer from the surface [47,48]. All of the excitation mechanisms enable control over reaction pathways of molecules on surfaces, offering new avenues for on-surface chemical reactions.

Hitherto, on-surface dechlorinated couplings rely on increasing temperatures to break the strong C-Cl bonds [29,33–35,49–52]. In this work, we aim to realize on-surface photo-induced dehalogenation reactions, focusing on the dechlorinated coupling reaction. We have achieved the dechlorination of three aryl chlorides on Au(111) under mild temperatures by photochemistry. The photon sources utilized in this study include a visible light at a wavelength of 405 nm and an ultraviolet (UV) light at 254 nm. The study shows that photochemistry holds great promise for advancing the surface chemistry of organic molecules and building

* Corresponding author.
E-mail address: qiangsun@shu.edu.cn (Q. Sun).

https://doi.org/10.1016/j.cclet.2024.109807
1001-8417/

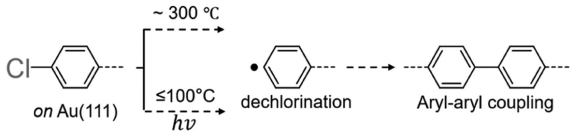

Fig. 1. Reaction scheme of the on-surface dechlorinated coupling *via* heating and photochemistry.

tailored nanostructures. We are aiming to accomplish the photo-induced dechlorination on Au(111), which is more challenging than debromination and deiodination due to the significantly higher activation energy required to break C-Cl bonds. Dechlorination is also a fundamental reaction with significant implications for environmental protection and sustainable chemistry [53]. Achieving thermal dechlorination typically requires high activation temperatures, ~670 K on Au(111) (schematically shown in Fig. 1) [33,34]. We have initially selected a chlorinated aromatic molecule, 2,7-dichloro-9-fluorenone ($C_{13}H_6Cl_2O$, shorted as DCF) as a model system. After depositing DCF onto Au(111) at room temperature, the molecule appears as a rod-like pattern on the surface in STM images (Fig. 2a). We can find two distinct self-assembled nanostructures of organized arrangement formed by the molecule, as illustrated by the STM images in Fig. S1 (Supporting information). One of the self-assembled nanostructures takes a windmill organization. The other self-assembled nanostructure exhibits a brick-wall pattern. The density functional theory (DFT) calculations suggest that the chlorine atoms on either side of the DCF molecule contribute to the stabilizations of the nanostructures (Figs. S1c and e).

Subsequently, we exposed the sample to a violet light at a wavelength of 405 nm. Fig. 2b illustrates that after light irradiation, a small amount of brick-type self-assembled arrangement appeared, which is different from the previous brick-wall pattern. Remarkably, our STM images reveal the presence of bright spots situated between each adjacent pair of molecules along the molecular longitudinal direction. This strip is indicative of the detached chlorine atoms, as previously observed after heat-induced dechlorination on the same surface [54]. We therefore infer that single-molecule dechlorination has taken place. Fig. 2c shows the corresponding molecular models. While, we also note that there is no sign of the polymerization between DCF molecules, as there is no change in the length of the products (1.3 ± 0.1 nm). This is likely rooted in the intrinsic chemical properties of the DCF molecule. In the following sections, we will show that the photo-induced reaction will result in polymerizations for other aryl chlorides. Additionally, the dissociation of the C=O bond is highly unlikely given that the carbon-oxygen bonding energy is higher than that of the carbon-chlorine.

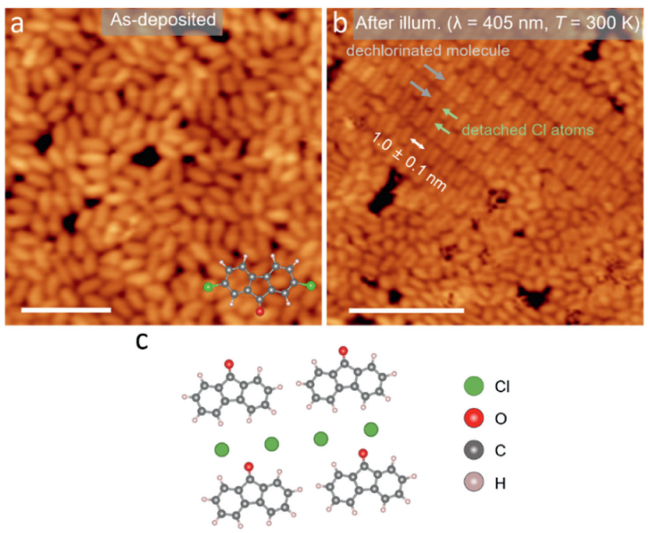

Fig. 2. Photo-induced dechlorination of DCF molecules. (a) STM image after depositing DCF molecules on Au(111) at room temperature ($V_s = -1.5$ V, $I_t = 100$ pA, scale bar: 4 nm). The chemical model of DCF is shown at the bottom right. (b) STM image after illuminating the DCF-covered sample with a violet light at 405 nm for 15 h at room temperature ($V_s = -1.8$ V, $I_t = 100$ pA, scale bar: 7 nm). Gray arrows depict dechlorinated DCF molecules, while the green arrows indicate the detached chlorine. White arrow represents the distance between adjacent molecules. (c) The molecular models corresponding to the dechlorinated brick-type self-assembled arrangement, where the green dots represent the chlorines.

Continuing our investigation on the impact of light on the dechlorination reaction, we explored the yield of the dechlorination against the duration of the light illumination. Although DCF also adopts a brick-wall self-assembly when heated to 375 K, STM measurements reveal that the intermolecular distance within this assembly is 0.5 ± 0.1 nm (Fig. S1d), which is less than that of around 1 nm observed in the brick-type self-assembled post-dechlorination (Fig. 2b). Therefore, we conclude that dechlorination does not occur when DCF is heated to 375 K without light illumination. After ensuring that no dechlorination reaction occurs in the sample at 375 K, we mildly heated the sample to 375 K for photoinduced dechlorination since the photoreaction rate is too low at room temperature to ensure reliable statistics. The typical STM images of the different samples at varying times of light exposure are displayed in Figs. 3a-d and Figs. S2-S4 (Supporting information). We manually counted the reacted molecules and unreacted molecules from the STM images (Fig. S5 in Supporting information). As indicated in Fig. 3e, a statistical analysis of the share of the dechlorinated molecules with the time of light illumination is plotted. As we increase the illumination duration, the fraction of molecules undergoing dechlorination gradually rises, which aligns well with our expectations. The consistent increase in the proportion of molecules experiencing chlorine detachment with extended exposure time reaffirms the validity of our hypothesis regarding the crucial role of light in driving the dechlorination process.

To explore the generality of the photo-induced dechlorination on metal surfaces, we have studied another aryl chloride of 4,4′-dichlorobiphenyl (Fig. 4a, henceforth shorted as DCBP). DCBP was initially deposited onto Au(111). The resulting STM image unveiled a characteristic herringbone-type arrangement of the molecules on the surface (Fig. 4b). Our DFT calculations support the alternating arrangement of DCBP stabilized through hydrogen bonding, thereby facilitating a notably dense molecular assembly (Fig. 4c). Our STM images reveal that the length of an individual DCBP molecule in STM images is 1.1 ± 0.1 nm. This measurement lays the ground for our subsequent analysis of the polymerization of this molecule.

Subsequently, the as-deposited sample was placed under the 405 nm light for as long as 43 h at room temperature. However, there was no evidence of dechlorination or oligomerization. We therefore mildly increased the surface temperature to 365 K and simultaneously illuminated the sample to the 405 nm light. Owing to the low molecular weight of DCBP molecules, a temperature increase results in their substantial desorption [55]. After about 8 h, the STM data unveiled the presence of short chains at the step edges of the substrate. Through careful measurements of their lengths, we determined the longest chain to be 6.0 ± 0.1 nm as pointed out by the white arrow in Fig. 4d, consistent with a pentamer. This observation strongly points to the dechlorination and the subsequent polymerization of the dechlorinated species. We speculate that the light-induced dechlorinated coupling after simultaneous heating and light exposure is due to the enhanced molecular mobility of the molecules.

Apart from using different molecular precursors, we also investigated the potential impact of light sources at different wave-

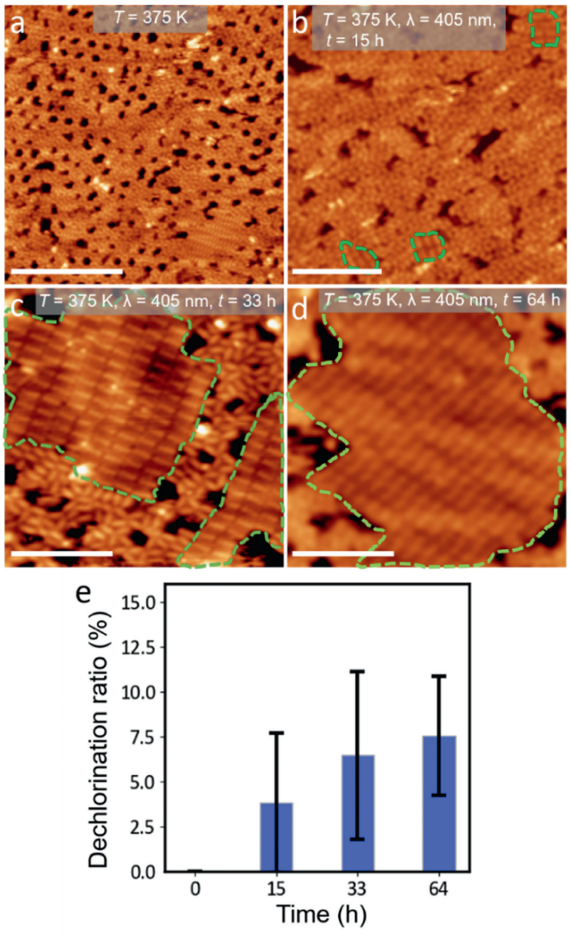

Fig. 3. The yield of the dechlorination against the duration of light illuminations. Representative STM images acquired (a) without light irradiation ($V_s = -1.8$ V, $I_t = 100$ pA, scale bar: 20 nm), (b) after 15 h of illumination ($V_s = -1.8$ V, $I_t = 100$ pA, scale bar: 10 nm), (c) 33 h of illumination ($V_s = -1.8$ V, $I_t = 100$ pA, scale bar: 10 nm) and (d) 64 h of illumination ($V_s = -1.8$ V, $I_t = 40$ pA, scale bar: 7 nm). The green dashed lines enclose the dechlorinated molecules. (e) Statistical analysis of the share of the dechlorinated molecules over light illumination time. We use the standard deviation as errors.

lengths on the dechlorination. The sample with pristine DCBP molecules on Au(111) was subjected to the illumination of a 254 nm UV light at room temperature. Analogous to the violet light at 405 nm, our STM measurements indicated that DCBP did not experience dechlorination or oligomerization. Consequently, we involved heating at 365 K and simultaneous light exposure to the 254 nm light. Finally, we observed extended molecular chains on the surface (Fig. 4e). Importantly, these chains were not just confined to the step edges, but also on the terrace. The longest chain was measured to be 4.9 ± 0.1 nm, matching the dimensions of a tetramer.

As compared to the heat-induced dehalogenated couplings [4,5], the introduction of light to induce on-surface reactions allows for dehalogenation and polymerization at much lower temperatures. The reduced temperature suppresses the molecular diffusions on the surface, resulting in the fabrication of shorter molecular chains. These findings may provide new fundamental details for understanding surface reaction kinetics and the elementary reactions along the reaction pathways.

We selected DCF and DCBP as the precursors of our research due to the presence of chlorine at both ends of these molecules. Finally, we decided to focus on a molecule with only one chlorine atom for our subsequent study. We performed the photo

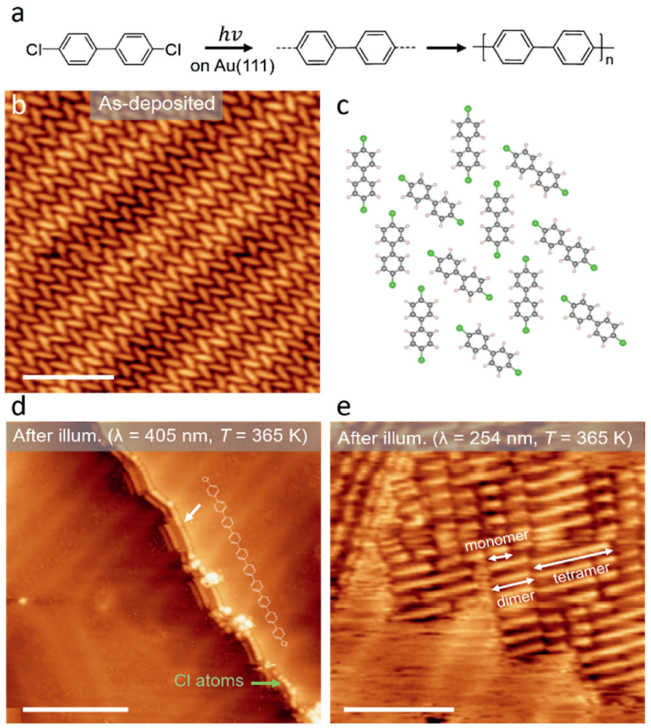

Fig. 4. Photo-induced dechlorination of DCBP molecules. (a) The reaction scheme. (b) STM image following the deposition of DCBP molecules on Au(111) at room temperature ($V_s = -1.8$ V, $I_t = 100$ pA, scale bar: 5 nm). (c) The DFT computed molecular model of the herringbone-type self-assembled arrangement in (b). (d) A representative STM image after shining the sample with a violet light at 405 nm at 365 K for 8 h ($V_s = -2.1$ V, $I_t = 50$ pA, scale bar: 10 nm). The formed oligomers are observed along the step edge. The longest chain consistent with a pentamer is indicated by the white arrow. The chlorine atoms are indicated by the green arrow. (e) A representative STM image obtained after irradiating with a 254 nm UV light at 365 K for 13.5 h ($V_s = -0.5$ V, $I_t = 200$ pA, scale bar: 7 nm).

reaction of another molecule with single chlorine functionalization, 4-chloro-5′-phenyl-1,1′:3′,1″-terphenyl (shorted as CPT) on the Au(111) surface. CPT consists of four benzene rings, and a single chlorine atom is exclusively positioned on the outer side enabling the dimerization (Fig. 5a). Fig. 5b shows the intact CPT molecule after deposition onto Au(111) at room temperature. We

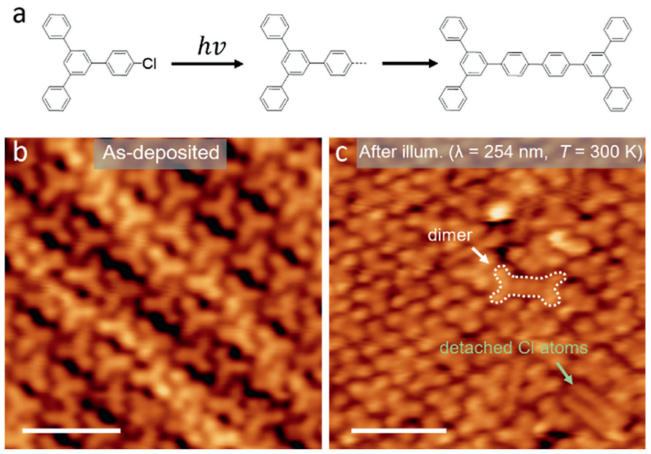

Fig. 5. Photo-induced dechlorination of CPT molecules. (a) The reaction scheme. (b) STM image following the deposition of CPT molecules onto Au(111) at room temperature ($V_s = -1.8$ V, $I_t = 100$ pA, scale bar: 3 nm). (c) STM image of the sample after irradiated by a 254 nm UV light for 12 h ($V_s = -2.0$ V, $I_t = 100$ pA, scale bar: 3 nm). The white dotted line indicates the formed dimer and the green arrow highlights the detached chlorine atoms.

then illuminated the sample with the 254 nm UV light for 12 h with the surface held at room temperature. The subsequent STM measurement unequivocally displayed evidence of dechlorination from the formation of a dog-bone-like dimer structure along with the detached chloride atoms among the molecules (Fig. 5c). Note that exposing the sample to a violet light at 405 nm leads to no dechlorination or polymerization of CPT molecules.

While our investigation has predominantly focused on the use of light to facilitate dechlorination at low temperatures, we recognize the need to deeply understand the surface reaction mechanisms involved. Our preliminary findings suggest that on Au(111) surfaces, the reaction pathway at 254 nm is likely dominated by the direct excitation of the molecules, while at 405 nm, surface hot electrons are believed to take effect [47].

In summary, we have investigated the dechlorination of aryl chlorides through on-surface photochemistry. By employing two different light sources, a violet light at 405 nm and an ultraviolet light at 254 nm, we have accomplished the Ullman-type dechlorination on the metal surfaces below or equivalent to 100 °C which would otherwise require around 300 °C without light activations. To demonstrate the generality of the photoinduced reaction, we have studied three different aryl chlorides and all of their C-Cl bonds can be broken *via* photoactivation under mild temperatures. These findings highlight the potential of photochemistry in achieving uncommon on-surface reactions. The formation of oligomers and monomers after the photo-induced dechlorination marks the distinct reaction scenarios of on-surface photochemistry, in contrast to the traditional heat-triggered on-surface reaction, offering an intriguing avenue for the atomically precise synthesis of unconventional nanomaterials.

Declaration of competing interest

The authors declare that they have no known competing financial interests or personal relationships that could have appeared to influence the work reported in this paper.

Acknowledgment

This work was supported by National Natural Science Foundation of China (Nos. 22072086, 22302120).

Supplementary materials

Supplementary material associated with this article can be found, in the online version, at doi:10.1016/j.cclet.2024.109807.

References

[1] N.R. Champness, Nat. Nanotech. 2 (2007) 671–672.
[2] Q. Shen, H.Y. Gao, H. Fuchs, Nano Today 13 (2017) 77–96.
[3] S. Song, J. Su, M. Telychko, et al., Chem. Soc. Rev. 50 (2021) 3238–3262.
[4] S. Clair, D.G. de Oteyza, Chem. Rev. 119 (2019) 4717–4776.
[5] L. Grill, S. Hecht, Nat. Chem. 12 (2020) 115–130.
[6] J. Björk, F. Hanke, S. Stafström, J. Am. Chem. Soc. 135 (2013) 5768–5775.
[7] J. Björk, C. Sánchez-Sánchez, Q. Chen, et al., Angew. Chem. Int. Ed. 61 (2022) e202212354.
[8] C. Ma, Z. Xiao, P.V. Bonnesen, et al., Chem. Sci. 12 (2021) 15637–15644.
[9] M. Lackinger, Chem. Commun. 53 (2017) 7872–7885.
[10] L. Lafferentz, F. Ample, H. Yu, et al., Science 323 (2009) 1193–1197.
[11] L. Grill, M. Dyer, L. Lafferentz, et al., Nat. Nanotechnol. 2 (2007) 687–691.
[12] H. Jiang, J. Lu, F. Zheng, et al., Chem. Commun. 59 (2023) 8067–8070.
[13] J. Eichhorn, D. Nieckarz, O. Ochs, et al., ACS Nano 8 (2014) 7880–7889.
[14] M. Di Giovannantonio, M. El Garah, J. Lipton-Duffin, et al., ACS Nano 7 (2013) 8190–8198.
[15] J. Cai, P. Ruffieux, R. Jaafar, et al., Nature 466 (2010) 470–473.
[16] C. Ma, J. Wang, H. Ma, et al., J. Am. Chem. Soc. 145 (2023) 10126–10135.
[17] D.Y. Li, X. Qiu, S.W. Li, et al., J. Am. Chem. Soc. 143 (2021) 12955–12960.
[18] R. Pawlak, X. Liu, S. Ninova, et al., J. Am. Chem. Soc. 142 (2020) 12568–12573.
[19] B. Cirera, A. Sánchez-Grande, B. de la Torre, et al., Nat. Nanotechnol. 15 (2020) 437–443.
[20] R.D. McCurdy, A. Delgado, J. Jiang, et al., J. Am. Chem. Soc. 145 (2023) 15162–15170.
[21] Y. Zhang, J. Lu, Y. Li, et al., Angew. Chem. Int. Ed. 61 (2022) e202204736.
[22] Q. Sun, H. Jiang, Y. Yan, R. Fasel, P. Ruffieux, Nano Res. 15 (2022) 8465–8469.
[23] Q. Sun, Y. Yan, X. Yao, et al., J. Phys. Chem. Lett. 12 (2021) 8679–8684.
[24] H. Zhang, J. Lu, Y. Zhang, et al., Chin. Chem. Lett. 34 (2023) 107450.
[25] F. Xiang, S. Maisel, S. Beniwal, et al., Nat. Chem. 14 (2022) 871–876.
[26] B. Yuan, C. Li, Y. Zhao, et al., J. Am. Chem. Soc. 142 (2020) 10034–10041.
[27] X. Zhu, Y. Liu, W. Pu, et al., ACS Nano 16 (2022) 10600–10607.
[28] M. Di Giovannantonio, X. Yao, K. Eimre, et al., J. Am. Chem. Soc. 142 (2020) 12046–12050.
[29] Q. Zhong, K. Niu, L. Chen, et al., J. Am. Chem. Soc. 144 (2022) 8214–8222.
[30] Z. Zeng, D. Guo, T. Wang, et al., J. Am. Chem. Soc. 144 (2022) 723–732.
[31] Q. Fan, L. Yan, M.W. Tripp, et al., Science 372 (2021) 852–856.
[32] F. Palmino, C. Loppacher, F. Chérioux, ChemPhysChem 20 (2019) 2271–2280.
[33] K.J. Shi, D.W. Yuan, C.X. Wang, et al., Org. Lett. 18 (2016) 1282–1285.
[34] F. Schulz, P.H. Jacobse, F.F. Canova, et al., J. Phys. Chem. C 121 (2017) 2896–2904.
[35] P.H. Jacobse, A. van den Hoogenband, M.E. Moret, R.J.M. Klein Gebbink, I. Swart, Angew. Chem. Int. Ed. 55 (2016) 13052–13055.
[36] S.W. Hla, L. Bartels, G. Meyer, K.H. Rieder, Phys. Rev. Lett. 85 (2000) 2777.
[37] Q. Zhong, A. Ihle, S. Ahles, et al., Nat. Chem. 13 (2021) 1133–1139.
[38] Y. Wang, M. Zhong, J. Li, et al., Chin. Chem. Lett. 33 (2022) 1074–1076.
[39] M. Zhong, Q. Wu, L. Ma, et al., Chin. Chem. Lett. 34 (2023) 107813.
[40] S. Clair, O. Ourdjini, M. Abel, L. Porte, Chem. Commun. 47 (2011) 8028–8030.
[41] C. Nacci, M. Schied, D. Civita, et al., J. Phys. Chem. C 125 (2021) 22554–22561.
[42] J.I. Urgel, S. Mishra, H. Hayashi, et al., Nat. Commun. 10 (2019) 861.
[43] H. Böckmann, S. Liu, J. Mielke, et al., Nano Lett. 16 (2016) 1034–1041.
[44] E. Kazuma, J. Jung, H. Ueba, M. Trenary, Y. Kim, J. Am. Chem. Soc. 139 (2017) 3115–3121.
[45] H.Y. Gao, D. Zhong, H. Mönig, et al., J. Phys. Chem. C 118 (2014) 6272–6277.
[46] A. Basagni, L. Ferrighi, M. Cattelan, et al., Chem. Commun. 51 (2015) 12593–12596.
[47] H. Jiang, Y. He, J. Lu, et al., ACS Nano 18 (2023) 1118–1125.
[48] E. Kazuma, J. Jung, H. Ueba, et al., Prog. Surf. Sci. 93 (2018) 163–176.
[49] J.C. Moreno-López, D.J. Mowbray, A. Pérez Paz, et al., Chem. Mater. 31 (2019) 3009–3017.
[50] R.C. de Campos Ferreira, A. Pérez Paz, D.J. Mowbray, et al., Phys. Chem. C 124 (2020) 14220–14228.
[51] R. Zuzak, P. Brandimarte, P. Olszowski, et al., J. Phys. Chem. Lett. 11 (2020) 10290–10297.
[52] G. Galeotti, M.D. Giovannantonio, J. Lipton-Duffin, et al., Faraday Discuss. 204 (2017) 453–469.
[53] B.Z. Wu, H.Y. Chen, S.J. Wang, et al., Chemosphere 88 (2012) 757–768.
[54] K.J. Shi, X. Zhang, C.H. Shu, et al., Chem. Commun. 52 (2016) 8726–8729.
[55] X. Zhou, F. Bebensee, Q. Shen, et al., Mater. Chem. Front. 1 (2017) 119–127.